

Analyzing the Impact of Additive and Multiplicative Noise on Seismic Data Analysis

Akshika Rohatgi*, Andrey Bakulin, and Sergey Fomel, Bureau of Economic Geology, The University of Texas at Austin

SUMMARY

Multiplicative noise presents a distinct challenge in image processing problems. While seismic noise has conventionally been considered additive noise, in recent years, multiplicative speckle noise has been recognized as caused by small-scale scattering in the near surface. We scrutinize multiplicative noise's phase and amplitude characteristics across time and frequency domains by extending the previous analysis to broadband data. Theoretical analysis and numerical experiments show that while stacking-based processing can effectively neutralize additive noise, it struggles against the complexities of multiplicative noise.

INTRODUCTION

When faced with complex near-surface conditions, single-sensor land seismic data often exhibit intricate noise patterns (Figure 1a). Employing local stacking techniques, whether via a geophone array in the field (Figure 1b) or during processing, significantly mitigates noise levels but at the cost of notable amplitude attenuation, particularly at higher frequencies. Bakulin et al. (2022) recognized that reflection distortions caused by small-scale scattering play a significant role in this complexity and introduced the notion of seismic speckle noise. This type of noise, akin to phenomena observed in optics and acoustics (Abbott and Thurstone, 1979); (Derode and Fink, 1998); (Goodman, 2007), distorts the signal through multiplicative factors, complicating the success of suppression efforts in preserving the signal integrity. Multiplicative noise with random perturbations is new to the seismic field, but this kind of phase perturbation is well-established in optics, acoustics, and ultrasonic imaging. Goodman (2007) established a multiplicative noise model, focusing on monochromatic speckle noise. Building upon this theoretical foundation, Bakulin et al. (2022) introduced a similar mathematical model tailored for broadband seismic traces characterized by general multiplicative noise, identifying two main forms: random phase perturbations and random time shifts (i.e., residual statistics).

Understanding both additive and multiplicative noise is critical for advancing seismic data analysis. In this paper, we aim to examine these noise's phase and amplitude impacts across time and frequency domains. Dissecting their influences and differentiating between different types of noise can help unravel the effect of noise on various signal processing techniques, notably stacking, an essential aspect of seismic signal processing and imaging.

We scrutinize amplitude and phase spectra changes to investigate the implications of noise perturbations on seismic signals. Additionally, we consider the role of stacking in mitigating noise effects and use simple numerical experiments to analyze residual phase distributions. Our objective is to refine the un-

derstanding of noise within seismic data analysis, employing data-driven diagnostics to distinguish between noise types and enhance seismic data processing strategies.

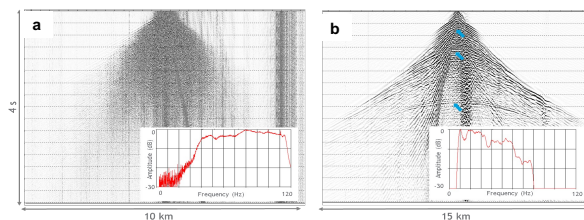


Figure 1: Field data recorded in a desert environment with (a) single sensors; and (b) with 72-geophone arrays (from Bakulin et al. (2022)).

NOISE MODELS

Additive noise model

This model introduces additive white noise to the seismic traces. The following formula represents a seismic trace $x_k(t)$ with noise:

$$x_k(t) = s(t) + n_k(t), \quad (1)$$

where $s(t)$ is the clean signal and $n_k(t)$ is the additive noise.

Multiplicative noise model

This model applies multiplicative noise to seismic traces within the Fourier domain as

$$X_k(\omega) = S(\omega) * R_k(\omega), \quad (2)$$

where $S(\omega)$ is the clean signal and $R_k(\omega)$ denotes the multiplicative noise. Equation (2) can model two types of multiplicative noise: random phase perturbations and random time shifts, with both assumed to follow a normal distribution akin to that observed in seismic field data, as follows:

$$R_k(\omega) = e^{i(\psi_k + \omega\tau_k)}. \quad (3)$$

Here, ψ_k represents phase perturbations varying independently across frequencies within a trace. This leads to complex signal changes of the ballistic arrivals in the time domain consistent with the field observations in complex regions. In contrast, residual statistics introduce linear phase shifts proportional to a constant time delay τ_k for each trace. We emphasize the crucial observation that both types of noise solely perturb the signal's phase in distinct ways while preserving the signal amplitude.

SIMULATING ADDITIVE VS MULTIPLICATIVE NOISE

We utilize numerical simulations to produce traces with a single Klauder wavelet, assembling 100 clean traces and modifying them by applying additive and multiplicative noise. Figure 2 showcases these ensembles, each comprising 100 traces

Additive and Multiplicative Noise

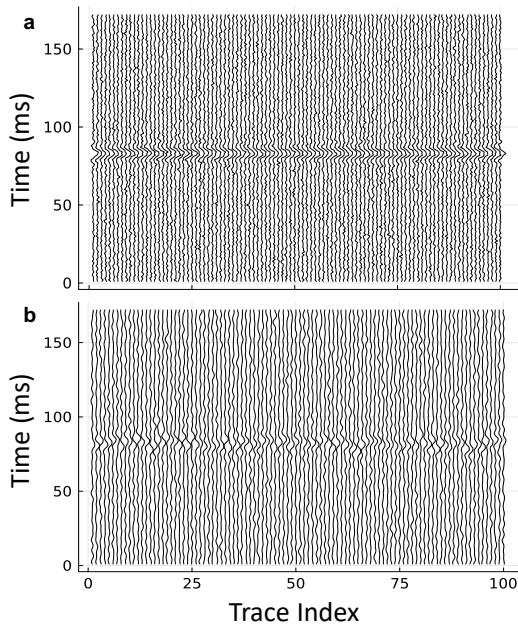


Figure 2: An ensemble of 100 traces affected by various noises, each with a consistent SNR of -1.2 dB: (a) traces with additive Gaussian noise; (b) traces with random multiplicative noise, characterized by standard deviations $\pi/3$ for phase perturbation and 4 ms for residual static. A Klauer wavelet represents the signal in each trace.

with an SNR of -1.2 dB for both noise types. Phase perturbations and residual statics follow a zero-mean normal distribution, with standard deviations of $\pi/3$ and 4 ms, respectively. These parameters ensure that the SNR, when calculated using the clean trace as the reference, matches the -1.2 dB noted in cases of additive noise, guaranteeing similar noise energy levels as illustrated in Figures 2a and 2b and providing a consistent basis for comparing the effects of these perturbations.

Signal in the time domain

Our initial analysis examines a single trace affected by both additive and multiplicative noise in the time domain, as depicted in Figure 3.

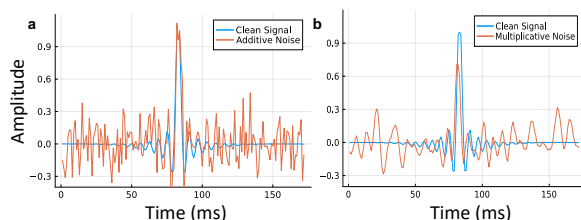


Figure 3: Noisy trace in the time domain, with the clean signal overlaid for comparison, showcasing the effects of (a) additive and (b) multiplicative noise.

Additive noise produces a uniform effect over time, leaving the position and energy of the central lobes slightly perturbed (Figure 3a), while multiplicative noise results in a varied impact, with mixed sporadic bursts and quieter regions (Figure 3b). Characteristically, multiplicative noise maintains the signal's overall energy ($|R| = 1$) but redistributes energy from the central lobe to other parts of the trace, resembling a scattering process.

We analyze the amplitude and phase in the frequency domain to delve deeper into noise characteristics.

Amplitude Spectra

Figure 4 illustrates the amplitude spectra for a single trace affected by each type of noise. Additive white noise modifies the amplitude spectrum, introducing peaks and valleys, resulting in an overall increase in average energy (signal plus noise) compared to the original signal. In contrast, multiplicative noise, affecting only the signal's phase, leaves the amplitude spectra unchanged before and after perturbations. Despite the significant reduction of the central lobe's energy (as seen in Figure 3b) suggesting attenuation, this apparent paradox is resolved when considering that complex phase adjustments merely redistribute energy within the time window, maintaining overall energy consistency.

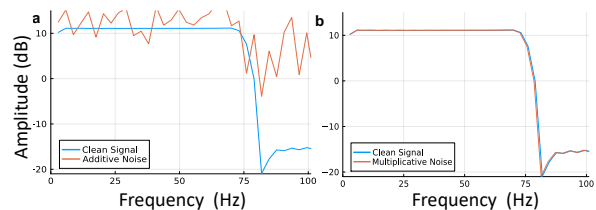


Figure 4: Amplitude spectra of a noisy trace, with the clean signal's spectra, overlaid in the Fourier domain for (a) additive and (b) multiplicative noise.

Phase Spectra

We analyze the phase distribution within the frequency domain for both types of noise, pre- and post-perturbation. Since multiplicative noise significantly impacts phase, understanding its effects is crucial. Figure 5 demonstrates that phase alterations due to multiplicative noise are more pronounced from low frequencies onwards. While statics introduce negligible changes at low frequencies, phase variations occur from these frequencies due to phase perturbations, which are assumed to have a constant standard deviation across the entire frequency band. In contrast, additive noise results in smaller deviations. Upon examining the wrapped residual phase difference between perturbed and clean signals, we find that both display symmetric, near-normal distributions at a fixed frequency (Figure 6). This phase spread is notably more pronounced with multiplicative than additive white noise, even when both have comparable SNRs. This is consistent with the observations presented in Figure 5.

Thus, an important conclusion from the statistical analysis of

Additive and Multiplicative Noise

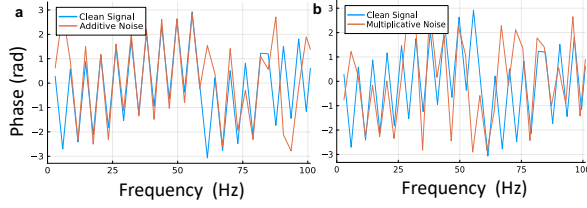


Figure 5: Wrapped phase spectra for noisy signals with clean signal overlays in the Fourier domain for (a) additive and (b) multiplicative noise.

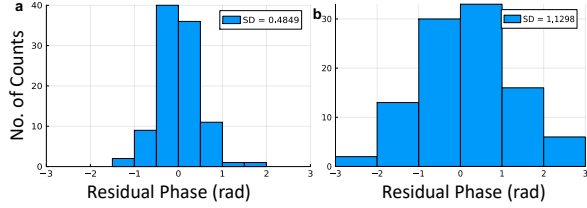


Figure 6: The residual phase distribution at 20 Hz across various noises: (a) shows the distribution for additive noise at an SNR of -1.2 dB, while (b) depicts the distribution for multiplicative noise attributed to phase perturbations with a standard deviation of $\sigma = \pi/3$, achieving a similar SNR of -1.2 dB.

the residual phase indicates that determining the type of noise affecting our data—be it additive or multiplicative—cannot be conclusively inferred from these distributions alone.

EFFECT OF LOCAL STACKING

The result of the local stacking of k traces in the frequency domain for additive noise is expressed as:

$$\hat{S}(\omega) = \frac{1}{k} \sum_{k=1}^k (S(\omega) + N_k(\omega)). \quad (4)$$

For a white Gaussian noise distribution, the mean of the noise components tends to zero with increasing N ,

$$\frac{1}{k} \sum_{k=1}^k N_k(\omega) = 0. \quad (5)$$

For multiplicative noise, local stacking is represented by the following equation:

$$\hat{S}(\omega) = \frac{1}{k} \sum_{k=1}^k (S(\omega) * R_k(\omega)). \quad (6)$$

Considering that τ_k and $\psi_k(\omega)$ are independent of each other and both random normally distributed with standard deviations σ_ψ and σ_τ , mathematical expectation of the stack can be written as (Bakulin et al., 2022)

$$E[S(\hat{\omega})] = |S(\omega)| e^{i\psi_s(\omega)} e^{-\frac{(\omega^2 \sigma_\tau^2)}{2}} e^{-\frac{\sigma_\psi^2}{2}}. \quad (7)$$

Significantly, stacking recovers the clean signal phase while attenuating the amplitudes due to residual statics and phase perturbation. Berni and Roever (1989) previously derived exponential loss $e^{-\frac{(\omega^2 \sigma_\tau^2)}{2}}$ analyzing intra-array residual statics without using a multiplicative noise model. To verify this effect numerically, we stack 100 traces perturbed by both types of noise and conduct further analysis in both time and frequency domains.

Stacked signal in the time domain

Consistent with the theoretical equations discussed earlier, stacking in the presence of additive noise yields a good approximation of the signal with only minor deviations, as illustrated in Figure 7a. On the other hand, stacking under multiplicative noise presents a more complex scenario. While the main lobes align well with the clean signal, indicating a successful signal recovery in phase, their energy is significantly attenuated, as depicted in Figure 7b. This attenuation presents substantial challenges, especially in practical situations with limited data, complicating the restoration of the original signal amplitude. This suggests that addressing speckle noise before stacking should emerge as an essential strategy for signal recovery in such contexts.

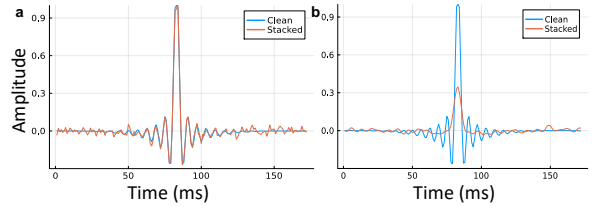


Figure 7: Stacked signal overlaid on the clean signal in the time domain for (a) additive and (b) multiplicative noise.

Amplitude Spectra

Figure 8 shows amplitude spectra after stacking to demonstrate the amplitude decay phenomenon. In the case of additive noise, we observe the restoration of distorted amplitude spectra, aligning with our expectations. In the case of multiplicative noise, we observe a drop in energy and escalating loss with frequency, consistent with equation (7). The observed difference in the multiplicative noise pattern can help us identify multiplicative noise in seismic data.

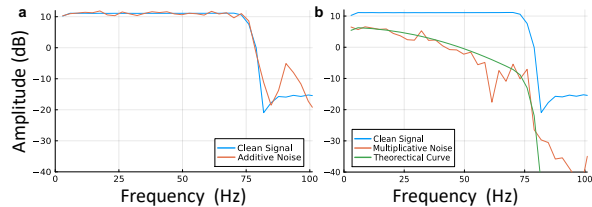


Figure 8: Amplitude spectra variation with frequency in Fourier domain after stacking for (a) additive and (b) multiplicative noise.

Additive and Multiplicative Noise

Phase Spectra

The phase spectra analysis post-stacking demonstrates effective phase recovery for both additive and multiplicative noise, as shown in Figure 9. The residual phases after stacking were further examined by repeating the process 100 times and calculating the residual phase against the original traces, yielding 100 realizations of the residual phase. This process reveals a significant reduction in the distribution of residual phases post-stacking. When comparing the residual phase distribution before and after stacking (refer to Figures 10 and 6), we observed a nearly tenfold decrease in spread for both types of noise, aligning with the expected $\frac{1}{\sqrt{N}}$ law. This analysis provided valuable insights into how stacking influences phase perturbations and contributes to signal restoration amidst additive and multiplicative noise.

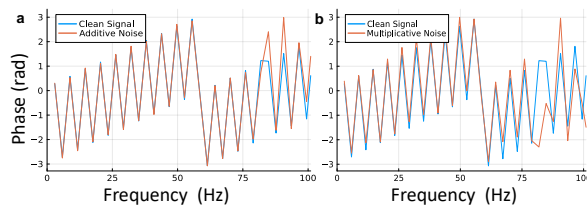


Figure 9: Wrapped phase spectra after stacking 100 noisy traces affected by (a) additive and (b) multiplicative noise, with the clean signal's phase shown for reference.

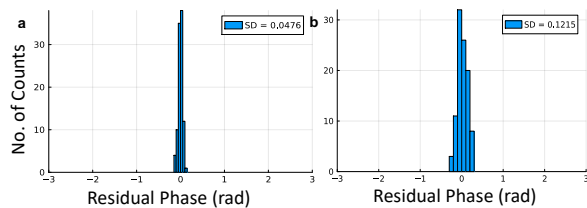


Figure 10: The residual phase distribution at 20 Hz post-stacking of 100 noisy traces impacted by (a) additive and (b) multiplicative noise.

Phasor Summation: An Intuitive Explanation

To decipher the impact of stacking on amplitude in the complex plane, we draw upon phasor summation, a concept previously used in speckle studies in optics, as discussed by Goodman (2007). Figure 11a demonstrates an initial vector at a specific frequency with amplitude A for the case of additive noise. Given that noise vectors are uniformly distributed in all directions, we consider them in pairs, such as N and $-N$, resulting in perturbed signals represented by vectors R_1 and R_2 . Summing these vectors forms a parallelogram (Figure 11a). The geometry of parallelograms, where diagonals bisect, means the total of vectors R_1 and R_2 is $2A$. Averaging these vectors leads to a return to amplitude A , illustrating that summing each noise vector pair preserves the original amplitude. By summing and normalizing all pairs, the stacking process consistently accu-

mulates the amplitude for the stacked signal, aligning with theoretical predictions for complete recovery without attenuation.

In contrast, multiplicative noise affects only the signal's phase, altering the vector by an angle θ that follows a symmetric normal distribution (equation 3) without changing amplitude. Considering noise vectors as pairs θ and $-\theta$, due to the symmetric nature of phase perturbations in multiplicative noise (Figure 11b), the combination of these vectors forms a rhombus with diagonal length $A(\sqrt{2+2\cos\theta})$. Averaging these vectors sum, as equation (6) indicates, the post-stacking amplitude consistently equals or is less than the original A , with greater θ leading to more attenuation. Summing all perturbed signal pairs results in a final stacked amplitude less than A , demonstrating attenuation increases with more significant phase perturbations, as described in equation (7).

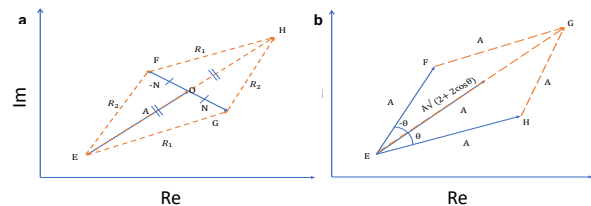


Figure 11: Stacked amplitude analysis through phasor summation in the complex plane for (a) additive and (b) multiplicative noise.

CONCLUSIONS

Our investigation into the difference between additive and multiplicative noises has illuminated their unique impacts on seismic signals and stacking-based processing. We have delineated the differences between these noise types, noting how they influence phase and amplitude spectra in both time and frequency domains. Our findings underscore that while stacking effectively neutralizes additive noise, it struggles against the complexities introduced by multiplicative noise.

Specifically, we demonstrated stacking's different capacities for recuperating the original signal's phase for both noise types. Numerical examples make it evident that local stacking cannot fully recover the original amplitude within the time domain, nor can it fully restore amplitude spectra in the frequency domain when dealing with multiplicative noise. This underscores the nuanced challenge multiplicative noise presents in seismic data analysis.

One can conclude that more sophisticated methodologies are needed for noise identification and tailored mitigation strategies for seismic land data processing in complex near-surface environments.

REFERENCES

- Abbott, J. G., and F. L. Thurstone, 1979, Acoustic speckle: theory and experimental analysis: *Ultrasonic Imaging*, **1**, 303–324, doi: <https://doi.org/10.1177/016173467900100402>.
- Bakulin, A., D. Neklyudov, and I. Silvestrov, 2022, Multiplicative random seismic noise caused by small-scale near-surface scattering and its transformation during stacking: *Geophysics*, **87**, no. 5, V419–V435, doi: <https://doi.org/10.1190/geo2021-0830.1>.
- Berni, A. J., and W. L. Roever, 1989, Field array performance: theoretical study of spatially correlated variations in amplitude coupling and static shift and case study in the Paris Basin: *Geophysics*, **54**, 451–459, doi: <https://doi.org/10.1190/1.1442671>.
- Derode, A., and M. Fink, 1998, Correlation length of ultrasonic speckle in anisotropic random media: Application to coherent echo detection: *The Journal of the Acoustical Society of America*, **103**, 73–82, doi: <https://doi.org/10.1121/1.421080>.
- Goodman, J. W., 2007, *Speckle phenomena in optics: Theory and applications*: Roberts and Company Publishers.